Triple Helix–Specific Ligands

J. L. Mergny, G. Duval-Valentin, C. H. Nguyen, L. Perrouault, B. Faucon, M. Rougée, T. Montenay-Garestier, E. Bisagni, C. Hélène*

A triple helix is formed upon binding of an oligodeoxynucleotide to the major groove of duplex DNA. A benzo[*e*]pyridoindole derivative (BePI) strongly stabilized this structure and showed preferential binding to a triplex rather than to a duplex. Energy transfer experiments suggest that BePI intercalates within the triple helix. Sequence-specific inhibition of transcription initiation of a specific gene by *Escherichia coli* RNA polymerase by a triplex-forming oligodeoxynucleotide is strongly enhanced when the triplex is stabilized by BePI. Upon irradiation with ultraviolet light, BePI induces covalent modifications of the target within the triple helix structure.

Homopyrimidine oligonucleotides can bind to the major groove of DNA at homopurine-homopyrimidine (*1*) sequences, forming a local triple helix (*1–3*). Sequence-specific binding in a parallel orientation to the purine strand rests upon Hoogsteen hydrogen bonds between thymine and T·A base pairs (T·A*T triplets) and between protonated cytosine and C·G base pairs (C·G*C^+ triplets) (*4, 5*). Triplex-forming oligonucleotides could interfere with transcription (6–9), which opens a new field of studies aimed at the design of sequence-specific gene regulators (*10*). However, triplex stability under physiological conditions appears somewhat limited; this limitation led to the design of chemical modifications that could increase the affinity of the third strand for its target (*11, 12*). One of the possibilities involves covalent linkage between an oligonucleotide and an intercalator that provides an additional binding energy (*11*).

In contrast to duplex DNA, little is known about the interaction of ligands with triple helices. Intercalators such as ethidium bromide interact with a triplex but with a lower affinity than for a duplex (*13, 14*). We report that a benzo[*e*]pyridoindole derivative (BePI, R = -OCH_3) (Fig. 1A) interacts more tightly with a triplex than with a duplex and strongly stabilizes the triplex structure, thus increasing its thermal stability by more than 20°C. BePI and a triple helix–forming oligonucleotide inhibit transcription of the β-lactamase gene by *E. coli* RNA polymerase in a cooperative manner. BePI induces covalent modifications of both Watson-Crick strands of the triplex upon irradiation with near-ultraviolet (near-UV) light. These adducts are observed at very low BePI concentrations (10 nM) and with high efficiency. These strong and specific binding sites disappear in the absence of the third oligonucleotide, which demonstrates a synergistic action of the chromophore and the oligonucleotide. Such triplex-specific ligands could be used to stabilize triplex structures under physiological conditions.

The density of negative charges around a T·A*T-rich triplex and the geometry of the base triplets led us to investigate the possibility of discovering triplex-specific cationic ligands that would have a higher affinity for a triple helix than for duplex DNA. Ethidium bromide interacts with a triplex structure, probably by intercalation (*13, 14*). Its lower affinity for a triplex in comparison to that for a duplex was demonstrated by a decrease in the thermal stability of the triple-stranded structure in the presence of the dye. However, a triplex-specific ligand should increase the melting temperature (T_m) of the triplex, displacing the equilibrium

$$\text{duplex} + \text{monomer} \rightleftarrows \text{triplex}$$

to the right; this phenomenon is observed with DNA ligands that bind weakly to single-stranded sequences and increase the T_m of the duplex (*15*). Several putative triplex ligands were investigated for their effects on the stability of various triplex structures, which differed by the relative number of T·A*T and C·G*C^+ triplets, as well as by their repartition in the sequence (Fig. 1B). Benzo[*e*]pyridoindole derivatives (Fig. 1A) were chosen because of their four planar rings that could optimize stacking between the dye and the triplets upon intercalation. The reference compound is BePI (Fig. 1A) (R = -OCH_3).

The kinetics of triple helix formation and dissociation were slow, which led to nonreversible melting curves in the absence of any dye (Fig. 2) (*16*). From an analysis of the melting curves obtained upon raising and decreasing temperature, an enthalpy ΔH of -70 ± 7 kcal/mol was calculated for the binding of the 14C3 oligonucleotide to a 26-bp duplex (Fig. 1B). Addition of increasing amounts of ethidium bromide decreased the thermal stability of the triplexes formed with the 14C3 and 14C5 oligonucleotides, as expected (*13, 14*). In contrast, concentration-dependent stabilization was induced by BePI, which led to a reversible melting curve for the 14C3 triplex with a T_m increase of 20°C with 15 μM BePI (Fig. 2A). From the thermodynamic parameters, a value of the free energy ΔG of -2.9 kcal/mol was calculated for the 14C3 triplex in the absence of BePI at 37°C, the melting temperature for the same triplex in the presence of BePI. At this temperature the apparent association constant (K_{ass}) for triplex formation in the presence of BePI is $1.3 \times 10^6\ M^{-1}$ ($\Delta G = -8.8$ kcal/mol; the triplex concentration was 1.5 μM, and at 37°C one-half of the third strand was dissociated). Thus, the binding of BePI provides an additional free energy of binding of -5.9 kcal/mol. This selective binding of BePI can therefore be used to increase triple helix stability, which appears to be limited under physiological conditions because of electrostatic repul-

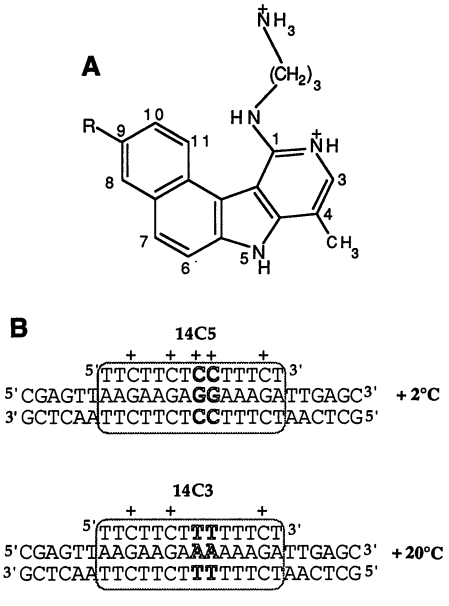

Fig. 1. (**A**) Structure of the compounds investigated. The most active tetracyclic compound (in terms of triplex stabilization) was the benzo[*e*]pyridoindole derivative with R = -OCH_3 in position 9 (BePI); its synthesis is described (*21*). (**B**) Sequence of two triplexes studied in this report. Stabilization of each triplex structure by BePI is expressed as a ΔT_{max} of the triplex-to-duplex transition with saturating concentrations of BePI (15 μM). See Fig. 2 for an example of melting curves obtained with the 14C3 oligonucleotide. The two structures differ by only two triplets (bold).

J. L. Mergny, G. Duval-Valentin, L. Perrouault, B. Faucon, M. Rougée T. Montenay-Garestier, C. Hélène, Laboratoire de Biophysique, Muséum National d'Histoire Naturelle, Institut National de la Santé et de la Recherche Médicale U201, Centre National de la Recherche Scientifique UA481, 43 rue Cuvier, 75005 Paris, France.
C. H. Nguyen and E. Bisagni, Laboratoire de synthèse organique, Institut Curie-Biologie, URA 1387 CNRS, Batiment 110, 91405 Orsay, France.
*To whom correspondence should be addressed.

sions between the duplex and the third strand and a requirement for protonated cytosine, which is unfavorable at a neutral pH. The stabilizing effect of BePI is much larger than that of a polycation such as spermine (*1, 11, 17*) (Fig. 2B).

A long stretch of T·A*T triplets was necessary for triple helix stabilization by BePI. When the triple helix contained six adjacent T·A*T triplets, the maximum T_m increase was 20°C (Fig. 1B). In contrast, stabilization of a 14-mer triplex (14C5) that contained no more than three contiguous T·A*T triplets was 2°C at a BePI concentration of 15 μM. An ellipticine derivative binds to the triplex-duplex junctions, especially on the 5′ side of the third strand (*18*). The binding of the two oligonucleotides 14C5 and 14C3 to their 26-bp duplex sequences (Fig. 1B) creates the same junctions, although the observed stabilization was very different (2° and 20°C, respectively), which indicates that BePI binds to the triplex region and not to the junctions.

Other triplex-forming oligonucleotides were investigated: (i) an 11-nucleotide (nt) sequence d5′(TTTCCTCCTCT)3′ whose triplex was stabilized only by 3°C; (ii) a 13-nt sequence d5′(CTTTTTCCTTCTC)3′ that formed a triplex that contained five adjacent T·A*T triplets and was stabilized by 10°C; and (iii) a 14-nt sequence d5′($T_{10}C_4$)3′, which formed a triplex that contained ten contiguous T·A*T triplets whose T_m was increased by more than 30°C. The presence of a stretch of adjacent T·A*T triplets appears to be critical for BePI preferential binding. This sequence preference can be explained by the presence of a positive charge in a C·G*C^+ triplet, which hampers the binding of a cationic dye such as BePI. These positive charges help determine the sequence specificity of binding of charged agents. A high density of negative charges was present at T·A*T stretches, which do not contain any positive charge.

The binding of BePI to a triplex induced hypochromic and bathochromic changes in absorption spectra (absorption maximum λ_{max} = 361 nm and extinction coefficient ϵ_{max} = 5500 M^{-1} cm^{-1} for free BePI; λ_{max} = 367 nm and ϵ_{max} = 4000 M^{-1} cm^{-1} for BePI bound to a triplex). The absorption and fluorescence excitation spectra of free BePI were identical, as expected from a single excited species. In contrast, a large difference between the excitation and absorption spectra of bound BePI was observed below 300 nm, as shown by the wavelength dependence of the fluorescence quantum yield of BePI (Fig. 3). The nucleic acid bases, the only other species absorbing at wavelengths below 300 nm, were responsible for the observed enhanced emission at 420 nm. Only excitation energy transfer from bases to BePI can account for these experimental results (*19*). Occurrence of fluorescence energy transfer from the base triplets to BePI can be considered as evidence for dye intercalation into the triplex, because the $1/r^6$ distance dependence of excitation energy transfer and the very low quantum yield of the bases (10^{-4} or less) give a very short Förster critical distance between the bases and BePI (*17, 19*). Competitive binding of ethidium bromide and BePI showed that BePI could easily displace ethidium from the triplex, which indicates that BePI affinity for the triplex was much higher than that of ethidium, which has a K_{ass} of 0.8 × 10^6 M^{-1} per site, as determined on a short triplex (*13*).

Oligonucleotides directed to a precise DNA sequence provide an interesting approach to artificially control the transcriptional process (*7, 10*). The *bla* gene from transposon Tn3 contains a 13-bp homopurine-homopyrimidine sequence located just downstream from the RNA polymerase binding site (positions +22 to +34, referring to the initiation site at +1). A 13-nt homopyrimidine oligonucleotide targeted to this sequence was tested for its effect on transcription of the β-lactamase gene in vitro (Fig. 4A). In the buffer (pH 7.8) used in our experiments, no footprint of 13C5 oligonucleotide on the homopurine-homopyrimidine region was observed at 25°C, even at 70 μM oligonucleotide concentration (Fig. 4B), showing that the triplex was not stable under these conditions probably because of the basic pH, which hampers cytosine protonation. In contrast, a clear footprint of this region was obtained upon simultaneous addition of BePI and 13C5 (Fig. 4B). This effect was correlated with a 10°C increase of the triplex-to-duplex T_m.

We used the cooperativity of binding of the oligonucleotide and BePI to inhibit the initiation of transcription of the β-lactamase gene by *E. coli* RNA polymerase (Fig. 4C). BePI alone had no effect on transcription at a concentration of 1.5 μM. Whereas the 13C5 oligonucleotide alone inhibited transcription by less than 10% at a concentration of 50 μM, a 70% inhibition was observed when both 13C5 (50 μM) and BePI (1.5 μM) were added. The consequence of the simultaneous presence of 13C5 and BePI was to block the holoenzyme at its start site. At pH 7.8, 13C5 alone was able to form only a loose complex with DNA and had a weak effect on transcription, even at high oligonucleotide concentration (*8*). Addition of BePI strength-

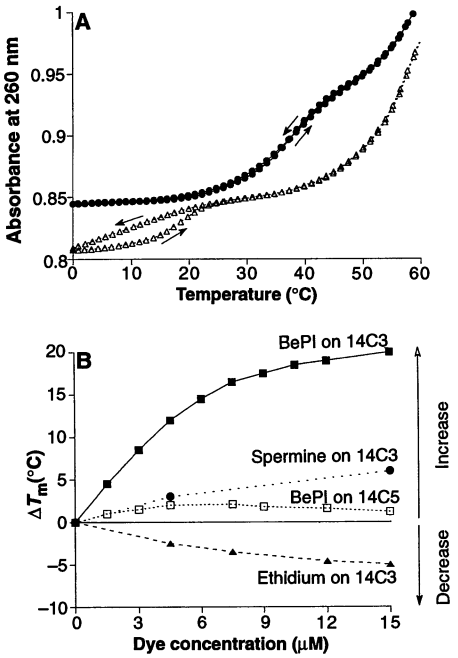

Fig. 2. (**A**) Denaturation profile of the 14C3 oligonucleotide (1.8 μM strand concentration) hybridized to a 26-bp double helix (1.5 μM) obtained in the absence (△) or in the presence (●) of 15 μM BePI. The denaturation profile for the triplex alone was not reversible, which shows that triplex formation was very slow with 0.1 M NaCl, 10 mM cacodylate (pH 6.2), and no spermine or magnesium. Arrows indicate the melting profiles when heating and cooling at a rate of 0.1°C per minute. (**B**) Modification of the denaturation temperature of the 14C3 triplex as a function of concentration for BePI (■), ethidium bromide (▲), and spermine (●) and of the 14C5 triplex as a function of BePI concentration (□). All experiments were performed in a 0.1 M NaCl and 10 mM cacodylate (pH 6.2) buffer.

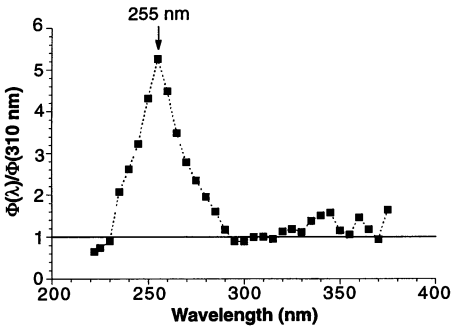

Fig. 3. Evidence for BePI intercalation into a triplex. BePI has a low fluorescence quantum yield (Φ < 0.01), but fluorescence measurements could still be performed at 1 μM dye concentration or higher. The apparent relative fluorescence quantum yield as a function of excitation wavelength is presented. This curve is the ratio between corrected excitation and absorption spectra of BePI (3 μM) bound to a triplex formed upon binding of 14C3 to a 14-bp duplex (3 μM strand concentration). Fluorescence intensities were normalized at an excitation wavelength of 310 nm where DNA bases do not absorb light. The experiment was performed at 0°C, with the 14C3 oligonucleotide fully hybridized to a 14-bp-long duplex. All experiments were performed in a 0.1 M NaCl and 10 mM cacodylate (pH 6.2) buffer. Emission was measured at 420 nm with a SPEX spectrofluorimeter.

ened the triplex and led to a much more efficient inhibition. No inhibition of transcription was observed on a different gene, governed by the *tetR* promoter of plasmid pSC101, which did not contain any binding site for 13C5. These results show that BePI and 13C5 did not alter the RNA polymerase itself but acted through triple helix formation.

All experiments described above were performed in the dark, and no irreversible modification of the triplex could be detected under these conditions. However, upon irradiation with near-UV light, BePI was able to induce covalent modifications of both strands of DNA when the triplex was formed with 14C3, as shown by denaturing gel electrophoresis (Fig. 5). Up to two molecules could be covalently linked to the same pyrimidine strand. More than 90% of the pyrimidine strand formed adducts with 100 nM BePI. Adducts were still observed with 10 nM BePI, provided that the third strand was present. Much higher concentrations of BePI were required to obtain measurable adducts in the absence of the third strand (Fig. 5). Similar adducts were observed on the 14C5 triplex but for higher BePI concentrations (a factor of 6 or greater), which suggests that the affinity of BePI for this triplex was lower, which is in agreement with the thermal denaturation experiments above. Monoadducts were observed on the purine strand, but with a lower efficiency (maximum yield of conversion was 50% at a BePI concentration of 300 nM). Treatment with piperidine (1 M at 95°C for 1 hour) after UV irradiation led to cleavage in the stretch of T·A*T triplets, which suggests that BePI binds inside the triplex and not at the duplex-triplex junctions as observed for an ellipticine derivative (*18*) or for other double helix intercalators (*20*). No modification of the target was observed with 10 nM BePI if the triplex site did not contain a stretch of adjacent T·A*T triplets.

In our experiments, we compared the affinity of different BePI derivatives. All of these molecules shared the same geometry—that is, four or three planar rings—but differed by the nature and location of substituents (*21–24*). Tricyclic analogs of BePI (pyridoindole derivatives that lacked the leftmost benzene ring shown in Fig. 1A) did not provide any stabilization of the triplex; instead, they destabilized it. In order to intercalate into a triplex, a dye must unstack two base triplets instead of two base pairs in duplex DNA, which would lead to a higher energy penalty (*25*). On the other hand, the intercalated dye might recover more binding energy by stacking with base triplets rather than with base pairs, depending on the size, shape, and location of its aromatic rings. This might explain why four rings are required for stabilization. The position of the methoxy group on the benzo ring was also shown to be critical: a methoxy group in position 10 or 8 induced a ΔT_m of 6°C and 4°C, respectively, as compared to a ΔT_m of 20°C for BePI (methoxy group at position 9). Replacement of the methoxy group in position 9 by a hydroxyl or by a hydrogen atom led to ΔT_m of 13°C and 3°C, respectively, as compared to a ΔT_m of 20°C for -OCH_3.

Some of the benzo[*e*]pyridoindole derivatives have been tested for antitumor activity in vitro on leukemic and solid tumor

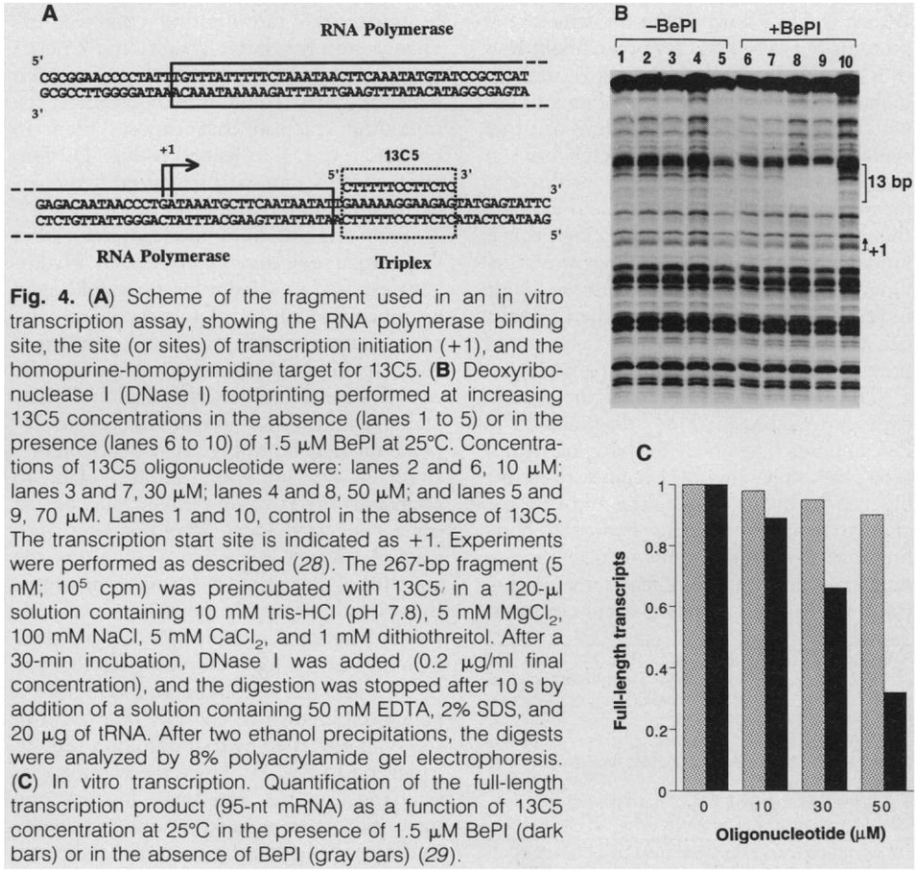

Fig. 4. (**A**) Scheme of the fragment used in an in vitro transcription assay, showing the RNA polymerase binding site, the site (or sites) of transcription initiation (+1), and the homopurine-homopyrimidine target for 13C5. (**B**) Deoxyribonuclease I (DNase I) footprinting performed at increasing 13C5 concentrations in the absence (lanes 1 to 5) or in the presence (lanes 6 to 10) of 1.5 μM BePI at 25°C. Concentrations of 13C5 oligonucleotide were: lanes 2 and 6, 10 μM; lanes 3 and 7, 30 μM; lanes 4 and 8, 50 μM; and lanes 5 and 9, 70 μM. Lanes 1 and 10, control in the absence of 13C5. The transcription start site is indicated as +1. Experiments were performed as described (*28*). The 267-bp fragment (5 nM; 10^5 cpm) was preincubated with 13C5 in a 120-μl solution containing 10 mM tris-HCl (pH 7.8), 5 mM $MgCl_2$, 100 mM NaCl, 5 mM $CaCl_2$, and 1 mM dithiothreitol. After a 30-min incubation, DNase I was added (0.2 μg/ml final concentration), and the digestion was stopped after 10 s by addition of a solution containing 50 mM EDTA, 2% SDS, and 20 μg of tRNA. After two ethanol precipitations, the digests were analyzed by 8% polyacrylamide gel electrophoresis. (**C**) In vitro transcription. Quantification of the full-length transcription product (95-nt mRNA) as a function of 13C5 concentration at 25°C in the presence of 1.5 μM BePI (dark bars) or in the absence of BePI (gray bars) (*29*).

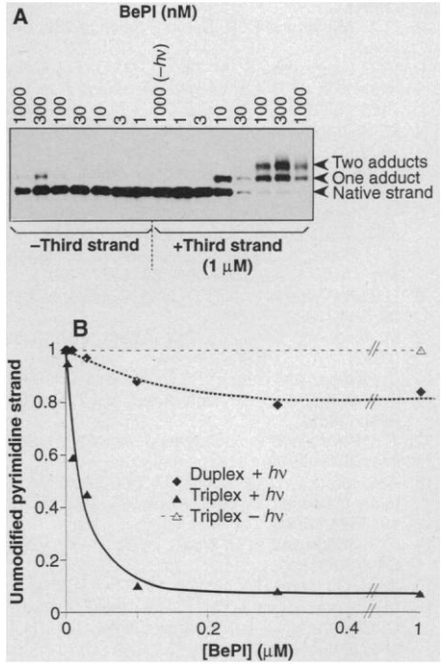

Fig. 5. (**A**) Photoinduced adducts of the homopyrimidine-containing strand of the 26-bp duplex (sequence as in Fig. 1B) as a function of BePI concentration from 1 to 1000 nM, in the presence (right) or in the absence (left) of the third strand 14C3 (1 μM). The center lane (where *hν* is the energy of the photon) is a control of the triple helix with BePI but without irradiation. The 26-bp duplex (10 nM) was incubated at 0°C with or without 14C3 and BePI for 12 hours, irradiated for 15 min at wavelength >300 nm, and then loaded on a denaturing 20% polyacrylamide–7 M urea gel. The pyrimidine strand of the 26-bp duplex was 5′-labeled. Bands corresponding to the unmodified (native) pyrimidine strand and the two products of BePI photoinduced addition are indicated at the right. Adding the dye without irradiation did not alter the migration of the control. (**B**) Fraction of unmodified pyrimidine strand of the 26-bp duplex as a function of BePI concentration in the absence (◆) and in the presence (▲) of the third strand 14C3. Irradiation conditions were as described in (A). The open triangle (△) corresponds to the nonirradiated triplex.

cells and in vivo on various experimental tumor models (*21*, *24*). They appear to be a promising new class of antineoplastic agents. One of their possible mechanisms of action involves interaction with topoisomerase II–DNA complexes (*21*). The experimental data presented here suggest that these drugs might also promote intramolecular triplex formation in vivo (such as by stabilizing H-DNA structures) and therefore might interfere with transcription and replication, which represents a new potential mechanism of action for these antitumor drugs.

REFERENCES AND NOTES

1. T. Le Doan, L. Perrouault, M. Chassignol, N. T. Thuong, C. Hélène, *Nucleic Acids Res.* **15**, 7749 (1987).
2. H. E. Moser and P. B. Dervan, *Science* **238**, 645 (1987).
3. V. I. Lyamichev, S. M. Mirkin, M. D. Frank-Kamenetskii, C. R. Cantor, *Nucleic Acids Res.* **16**, 2165 (1988).
4. P. Rajagopal and J. Feigon, *Biochemistry* **28**, 7859 (1989).
5. C. de los Santos, M. Rosen, D. Patel, *ibid.*, p. 7282.
6. M. Cooney, G. Czernuszewicz, E. H. Postel, S. J. Flint, M. E. Hogan, *Science* **241**, 456 (1988).
7. E. H. Postel, S. J. Flint, D. J. Kessler, M. E. Hogan, *Proc. Natl. Acad. Sci. U.S.A.* **88**, 8227 (1991).
8. G. Duval-Valentin, N. T. Thuong, C. Hélène, *ibid.* **89**, 504 (1992).
9. M. Grigoriev *et al.*, *J. Biol. Chem.* **267**, 3389 (1992).
10. C. Hélène, *Anti-Cancer Drug Des.* **6**, 569 (1991).
11. J. S. Sun *et al.*, *Proc. Natl. Acad. Sci. U.S.A.* **86**, 9198 (1989).
12. T. J. Povsic and P. B. Dervan, *J. Am. Chem. Soc.* **111**, 3059 (1989).
13. J. L. Mergny, D. A. Collier, M. Rougée, T. Montenay-Garestier, C. Hélène, *Nucleic Acids Res.* **19**, 1521 (1991).
14. P. V. Scaria and R. H. Shafer, *J. Biol. Chem.* **266**, 5417 (1991).
15. D. M. Crothers, *Biopolymers* **10**, 2147 (1971).
16. M. Rougée, B. Faucon, J. L. Mergny, F. Barcelo, C. Giovanangeli, T. Montenay-Garestier, C. Hélène, unpublished results.
17. J. P. Morgan and M. Daniels, *Photochem. Photobiol.* **31**, 101 (1980).
18. L. Perrouault *et al.*, *Nature* **344**, 358 (1990).
19. M. A. Sari, J. P. Battioni, D. Mansuy, J. B. Le Pecq, *Biochem. Biophys. Res. Commun.* **141**, 643 (1986).
20. D. A. Collier, J. L. Mergny, N. T. Thuong, C. Hélène, *Nucleic Acids Res.* **19**, 4219 (1991).
21. C. H. Nguyen, F. Lavelle, J. F. Riou, M. C. Bissery, C. Huel, E. Bisagni, *Anti-Cancer Drug Des.*, in press.
22. E. Bisagni *et al.*, *J. Med. Chem.* **31**, 398 (1988).
23. C. H. Nguyen, E. Bisagni, O. Pepin, A. Pierré, P. de Cointet, *ibid.* **30**, 1642 (1987).
24. C. H. Nguyen, J. M. Lhoste, F. Lavelle, M. C. Bissery, E. Bisagni, *ibid.* **33**, 1519 (1990).
25. T. Montenay-Garestier *et al.*, in *Molecular Basis of Specificity in Nucleic Acid-Drug Interactions*, B. Pullman and J. Jortner, Eds. (Kluwer Academic, Dordrecht, The Netherlands, 1990), pp. 275–291.
26. G. Duval-Valentin and R. Ehrlich, *Nucleic Acids Res.* **15**, 575 (1987).
27. R. R. Burgess and J. J. Jendrisak, *Biochemistry* **19**, 4639 (1975).
28. G. Duval-Valentin and R. Ehrlich, *Nucleic Acids Res.* **16**, 2031 (1988).
29. Transcription assays were performed in a 100 mM NaCl, 10 mM $MgCl_2$ (pH 7.8), and 10 mM tris-HCl buffer, with 5 nM of a 267-bp Eco RI–Hph I fragment carrying the *bla* promoter from plasmid pBR322. *Escherichia coli* RNA polymerase [45% active molecules (*26*) prepared as described (*27*)] was added in a 120-μl transcription buffer and incubated for 45 min at 37°C in order to obtain a maximum of open complexes, which are unstable when the incubation is performed directly at a lower temperature (*26*, *28*). After preincubation, aliquots of 10 μl were withdrawn and distributed into 12 tubes that contained heparin at 150 μg/ml (final concentration) to remove all nonspecific complexes and to trap all free polymerases. After 1 min, the incubation was continued at 25°C. The oligonucleotide was added at increasing concentrations in the presence or absence of 1.5 μM BePI, and the mixture was incubated for 30 min. The four ribonucleotides were then added [adenosine 5′-triphosphate, guanosine 5′-triphosphate, and cytidine 5′-triphosphate at 500 μM and uridine 5′-triphosphate (UTP) at 10 μM including [α-^{32}P]UTP at 20 Ci/mmol], and the elongation was stopped after 10 min by the addition of 4 μl of a solution containing 50 mM EDTA, 2% SDS, and 20 μg tRNA. After two ethanol precipitations, the transcripts were heated for 2 min at 90°C and loaded on a 20% denaturing polyacrylamide gel.

30. Supported by a grant from Rhône-Poulenc-Rorer and the Institute de Formation BioMédicale (J.L.M.). We thank O. Delgado for photography. Constant support by P. L. Dalton made this work possible. Supported in part by the Ligue Nationale Française Contre le Cancer.

15 January 1992; accepted 13 April 1992

Hydrogen Exchange Measurement of the Free Energy of Structural and Allosteric Change in Hemoglobin

S. Walter Englander,* Joan J. Englander, Russell E. McKinnie, Gary K. Ackers, George J. Turner, Judy A. Westrick, Stanley J. Gill

The inability to localize and measure the free energy of protein structure and structure change severely limits protein structure-function investigations. The local unfolding model for protein hydrogen exchange quantitatively relates the free energy of local structural stability with the hydrogen exchange rate of concerted sets of structurally related protons. In tests with a number of modified hemoglobin forms, the loss in structural free energy obtained locally from hydrogen exchange results matches the loss in allosteric free energy measured globally by oxygen-binding and subunit dissociation experiments.

Much is now known about the structure of proteins but very little is known about how they work. In working proteins such as hemoglobin (Hb), structural changes convert the energy of ligand binding or other sources into a functionally useful form. It has not before been possible to localize and measure structural free energy and changes therein in any general way although this is fundamental for understanding structure-function relations. Results presented here indicate that measurement of the normally occurring hydrogen exchange behavior of proteins can provide this information.

The local unfolding model for protein hydrogen exchange (HX), diagrammed in Fig. 1, holds that slowly exchanging hydrogens are slow simply because they are blocked by hydrogen bonding and that exchange requires transient hydrogen bond breakage (*1*), which tends to occur in cooperative local unfolding reactions (*2*). Local unfolding and refolding occur constantly. Since the rate-limiting chemical exchange step is relatively slow, the kinetics of exchange of a set of peptide group NHs depends on the equilibrium constant of the unfolding reaction that exposes them to exchange (Eq. 1 in legend to Fig. 1). This connects HX rate with structural free energy [(*2*); see Eq. 2 in legend to Fig. 1].

From the unfolding model, some rather surprising predictions can be drawn. Hydrogens exposed to solvent by the unfolding of a cooperative structural unit should all tend to exchange at similar rates, independent of their relative exposure to solvent in the native state. However, chemical and physical mechanisms can operate to obscure this behavior (legend to Fig. 1). Deeper predictions of the unfolding model relate to change in the HX rate of hydrogens placed on a concerted local unfolding unit (unfoldon). When a modification alters the stability of a protein, this can be measured in a global, reversible denaturation experiment. The same modification will produce a change in the local unfolding equilibrium of any affected unfoldon and therefore a concerted change in the HX rate of all of the NHs governed by that unfoldon (Eq. 2b in legend to Fig. 1). Thus, measurement of a change in HX rate may localize and quantify a change in structural free energy that must otherwise be measured indirectly

S. W. Englander, J. J. Englander, R. E. McKinnie, The Johnson Research Foundation, Department of Biochemistry and Biophysics, University of Pennsylvania, Philadelphia, PA 19104–6059.
G. K. Ackers and G. J. Turner, Department of Biochemistry and Molecular Biophysics, Washington University, St. Louis, MO 63110.
J. A. Westrick and S. J. Gill, Department of Biochemistry, University of Colorado, Boulder, CO 80309.
*To whom correspondence should be addressed.